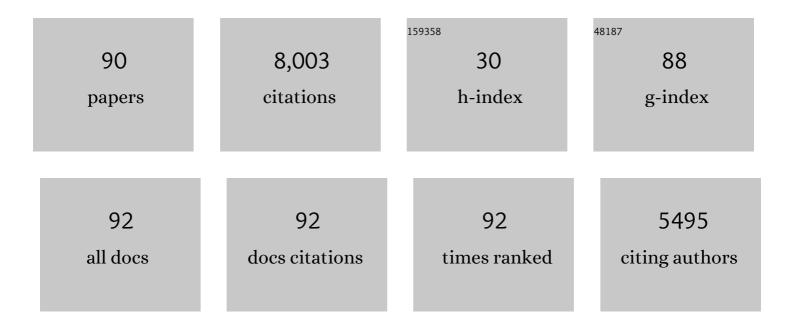
List of Publications by Year in descending order

Source: https://exaly.com/author-pdf/1468518/publications.pdf Version: 2024-02-01



#	Article	IF	CITATIONS
1	Conventional superconductivity at 203 kelvin at high pressures in the sulfur hydride system. Nature, 2015, 525, 73-76.	13.7	1,835
2	Electronic and magnetic phase diagram of β-Fe1.01Se with superconductivity at 36.7 K underÂpressure. Nature Materials, 2009, 8, 630-633.	13.3	943
3	Single-bonded cubic form of nitrogen. Nature Materials, 2004, 3, 558-563.	13.3	797
4	Transparent dense sodium. Nature, 2009, 458, 182-185.	13.7	710
5	Crystal structure of the superconducting phase of sulfur hydride. Nature Physics, 2016, 12, 835-838.	6.5	392
6	Superconductivity in Hydrogen Dominant Materials: Silane. Science, 2008, 319, 1506-1509.	6.0	340
7	Conductive dense hydrogen. Nature Materials, 2011, 10, 927-931.	13.3	303
8	Anomalous Highâ€Temperature Superconductivity in YH ₆ . Advanced Materials, 2021, 33, e2006832.	11.1	196
9	Superconductivity at 161â€ [–] K in thorium hydride ThH10: Synthesis and properties. Materials Today, 2020, 33, 36-44.	8.3	187
10	Structural transformation of molecular nitrogen to a single-bonded atomic state at high pressures. Journal of Chemical Physics, 2004, 121, 11296.	1.2	180
11	Polymerization of nitrogen in sodium azide. Journal of Chemical Physics, 2004, 120, 10618-10623.	1.2	146
12	Pressure-Induced Hydrogen-Dominant Metallic State in Aluminum Hydride. Physical Review Letters, 2008, 100, 045504.	2.9	136
13	Observation of superconductivity in hydrogen sulfide from nuclear resonant scattering. Science, 2016, 351, 1303-1306.	6.0	121
14	Superconductivity at 253â€ [–] K in lanthanum–yttrium ternary hydrides. Materials Today, 2021, 48, 18-28.	8.3	119
15	The strength of diamond. Applied Physics Letters, 2005, 87, 141902.	1.5	80
16	Single-crystalline polymeric nitrogen. Applied Physics Letters, 2007, 90, 171904.	1.5	73
17	Ammonia as a case study for the spontaneous ionization of a simple hydrogen-bonded compound. Nature Communications, 2014, 5, 3460.	5.8	70
18	Evidence of maximum in the melting curve of hydrogen at megabar pressures. JETP Letters, 2009, 89, 174-179.	0.4	69

#	Article	IF	CITATIONS
19	Molecular Structure of Hydrazoic Acid with Hydrogen-Bonded Tetramers in Nearly Planar Layers. Journal of the American Chemical Society, 2011, 133, 12100-12105.	6.6	69
20	Superconductivity in La and Y hydrides: Remaining questions to experiment and theory. Matter and Radiation at Extremes, 2020, 5, .	1.5	61
21	Excited states and selection rules in self-assembled InAs/GaAs quantum dots. Physical Review B, 1999, 60, R2185-R2188.	1.1	60
22	Phase stability of lithium azide at pressures up to 60 GPa. Journal of Physics Condensed Matter, 2009, 21, 195404.	0.7	58
23	High Pressure Synthesis of Marcasite-Type Rhodium Pernitride. Inorganic Chemistry, 2014, 53, 697-699.	1.9	55
24	Insulator-Metal Transition in Highly Compressed NiO. Physical Review Letters, 2012, 109, 086402.	2.9	53
25	Electronic and structural transitions in NdFeO3 orthoferrite under high pressures. JETP Letters, 2003, 77, 619-624.	0.4	40
26	Non-Traditional Carbon Semiconductors Prepared from Fullerite C60 and Carbyne under High Pressure. Physica Status Solidi (B): Basic Research, 1999, 211, 401-412.	0.7	39
27	Pressure induced polymorphism in ammonium azide (NH4N3). Chemical Physics, 2011, 386, 41-44.	0.9	37
28	Equation of state and structural transition at high hydrostatic pressures in the BiFeO3 crystal. JETP Letters, 2007, 86, 197-201.	0.4	34
29	Stable solid and aqueous H2CO3 from CO2 and H2O at high pressure and high temperature. Scientific Reports, 2016, 6, 19902.	1.6	34
30	Novel Strongly Correlated Europium Superhydrides. Journal of Physical Chemistry Letters, 2021, 12, 32-40.	2.1	33
31	The mechanism of suppression of strong electron correlations in FeBO3 at high pressures. Journal of Experimental and Theoretical Physics, 2004, 99, 566-573.	0.2	32
32	Magnetic collapse and the change of electronic structure of FeBO3 antiferromagnet under high pressure. JETP Letters, 2002, 76, 664-669.	0.4	30
33	Elastic properties of superhard amorphous carbon pressure-synthesized fromC60by surface Brillouin scattering. Physical Review B, 2001, 64, .	1.1	29
34	Superconductivity and equation of state of lanthanum at megabar pressures. Physical Review B, 2020, 102, .	1.1	29
35	Interplay between the structure and properties of new metastable carbon phases obtained under high pressures from fullerite C60 and carbyne. JETP Letters, 2002, 76, 681-692.	0.4	28
36	Transport and optical properties of iron borate FeBO3 under high pressures. JETP Letters, 2003, 78, 13-16.	0.4	28

#	Article	IF	CITATIONS
37	High-Pressure Magnetic Properties and P–T Phase Diagram of Iron Borate. Journal of Experimental and Theoretical Physics, 2005, 100, 688.	0.2	28
38	Nitrogen Backbone Oligomers. Scientific Reports, 2015, 5, 13239.	1.6	28
39	High-spin-low-spin transition in magnesiowüstite (Mg0.75,Fe0.25)O at high pressures under hydrostatic conditions. JETP Letters, 2010, 90, 617-622.	0.4	24
40	Normal and grazing incidence pulsed laser deposition of nanostructured MoS hydrogen evolution catalysts from a MoS2 target. Optics and Laser Technology, 2018, 102, 74-84.	2.2	24
41	Magnetic collapse in yttrium iron garnet Y3Fe5O12 at high pressure. JETP Letters, 2005, 82, 702-707.	0.4	23
42	Equation of state and structural phase transition in FeBO3 at high pressure. JETP Letters, 2002, 75, 23-25.	0.4	22
43	Exotic magnetism in the alkali sesquioxidesRb4O6andCs4O6. Physical Review B, 2009, 79, .	1.1	22
44	Transition from the antiferromagnetic to a nonmagnetic state in FeBO3 under high pressure. JETP Letters, 2001, 74, 24-27.	0.4	21
45	Irreversible electronic transition with possible metallization in Y3Fe5O12 at high pressure. JETP Letters, 2005, 82, 603-608.	0.4	20
46	Equation of state and high-pressure irreversible amorphization in Y3Fe5O12. JETP Letters, 2006, 83, 37-41.	0.4	20
47	Infrared study of hydrogen up to 310ÂGPa at room temperature. High Pressure Research, 2013, 33, 377-380.	0.4	20
48	Time for quartet: the stable 3 : 1 cocrystal formulation of FTDO and BTF – a high-energy-density material. CrystEngComm, 2020, 22, 4823-4832.	1.3	20
49	Pressure-tuned vibrational resonance coupling of intramolecular fundamentals in ammonium azide (NH4N3). Vibrational Spectroscopy, 2012, 58, 188-192.	1.2	17
50	Transformation from molecular to polymeric nitrogen at high pressures and temperatures: <i>In situ</i> x-ray diffraction study. Applied Physics Letters, 2008, 93, .	1.5	16
51	Measurement of the temperature distribution on the surface of the laser heated specimen in a diamond anvil cell system by the tandem imaging acousto-optical filter. High Pressure Research, 2019, 39, 131-149.	0.4	16
52	Pressure induced ionic-superionic transition in silver iodide at ambient temperature. Journal of Chemical Physics, 2014, 140, 044708.	1.2	14
53	MULTI-SPECTRAL IMAGE PROCESSING FOR THE MEASUREMENT OF A SPATIAL TEMPERATURE DISTRIBUTION ON THE SURFACE OF A LASER-HEATED MICROSCOPIC OBJECT. Computer Optics, 2017, 41, 864-868.	1.3	14
54	Anharmonicity of short-wavelength acoustic phonons in silicon at high temperatures. JETP Letters, 2000, 72, 195-198.	0.4	13

#	Article	IF	CITATIONS
55	Title is missing!. , 2000, 126, 305-311.		13
56	The magnetic P-T phase diagram of langasite Ba3TaFe3Si2O14 at high hydrostatic pressures up to 38 GPa. Applied Physics Letters, 2013, 103, 162402.	1.5	13
57	The effect of high pressure on the structure and on the magnetic and electronic properties of nickel monoxide. Journal of Experimental and Theoretical Physics, 2001, 92, 696-700.	0.2	10
58	Superconductivity and structural studies of highly compressed hydrogen sulfide. Physica C: Superconductivity and Its Applications, 2018, 552, 27-29.	0.6	10
59	Optical transitions in GdFe3(BO3)4 and FeBO3 under high pressures. Journal of Physics Condensed Matter, 2005, 17, 7599-7604.	0.7	9
60	High-pressure study of tetramethylsilane by Raman spectroscopy. Journal of Chemical Physics, 2012, 136, 024503.	1.2	9
61	Electronic structure of InAs–GaAs self-assembled quantum dots studied by perturbation spectroscopy. Physica E: Low-Dimensional Systems and Nanostructures, 2000, 6, 348-357.	1.3	8
62	Electron transport in FeBO3 ferroborate at ultrahigh pressures. JETP Letters, 2012, 94, 748-752.	0.4	8
63	Lone-pair interactions and photodissociation of compressed nitrogen trifluoride. Journal of Chemical Physics, 2014, 141, 064706.	1.2	8
64	Structural Transitions in Elemental Tin at Ultra High Pressures up to 230 GPa. JETP Letters, 2017, 106, 733-738.	0.4	8
65	Simultaneous measurements of the two-dimensional distribution of infrared laser intensity and temperature in a single-sided laser-heated diamond anvil cell. Comptes Rendus - Geoscience, 2019, 351, 286-294.	0.4	8
66	Excited States in Self-Assembled InAs/GaAs Quantum Dots under High Pressure. Physica Status Solidi (B): Basic Research, 1999, 211, 73-77.	0.7	7
67	Effect of high pressures on exchange and hyperfine interactions in rare-earth orthoferrites. Journal of Experimental and Theoretical Physics, 2000, 90, 330-340.	0.2	7
68	Equation of state and structural phase transitions in iron-based Ba3TaFe3Si2O14 langasite at high hydrostatic pressures. JETP Letters, 2015, 100, 798-806.	0.4	7
69	Structural Phase Transitions and the Equation of State in SnSe at High Pressures up to 2 Mbar. JETP Letters, 2018, 108, 414-418.	0.4	6
70	High pressure magnetic, structural, and electronic transitions in multiferroic Ba3NbFe3Si2O14. Applied Physics Letters, 2018, 112, 242405.	1.5	6
71	Pressureâ€Tuned Resonance Raman Scattering in InAs/GaSb Superlattices. Physica Status Solidi (B): Basic Research, 1996, 198, 321-327.	0.7	5
72	Magnetic phase separation and strong enhancement of the Néel temperature at high pressures in a new multiferroic Ba3TaFe3Si2O14. JETP Letters, 2017, 105, 26-33.	0.4	5

#	Article	IF	CITATIONS
73	Combined laser heating and tandem acousto-optical filter for two-dimensional temperature distribution on the surface of the heated microobject. Journal of Physics: Conference Series, 2018, 946, 012085.	0.3	5
74	The Effect of Boron on the Structure and Conductivity of Thin Films Obtained by Laser Ablation of Diamond with Deposition at 700°C. Technical Physics Letters, 2018, 44, 511-514.	0.2	5
75	Resonant Raman scattering in superconducting Ba1â^'x KxBiO3. JETP Letters, 2003, 77, 521-525.	0.4	4
76	Synthesis, Characterization of Elastic and Electrical Properties of Diamond-like BCx Nano-Phases Synthesized under High and Low Pressures. MRS Advances, 2018, 3, 45-52.	0.5	4
77	Reactions of nitronium sulfates: Hunting for dinitro sulfate. Journal of Raman Spectroscopy, 2019, 50, 1753-1762.	1.2	4
78	Studies of magnetic and optic properties of rare-earth gallo-ferroborates by MA¶ssbauer and optical spectroscopy. Physica B: Condensed Matter, 2005, 359-361, 1321-1323.	1.3	3
79	An imaging spectroradiometry system for measuring spatial temperature distributions in microscopic objects. Instruments and Experimental Techniques, 2017, 60, 401-406.	0.1	3
80	Structural phase transitions and the equation of state of SnTe at high pressures up to 2 mbar. JETP Letters, 2017, 106, 662-666.	0.4	3
81	Synthesis of New Materials in the Boron–Carbon System. Glass and Ceramics (English Translation of) Tj ETQo	110.7843 0.2	314 ₃ rgBT /Ov
82	Bonding, elastic and vibrational properties in low and high pressure synthesized diamond-like BCx phases. Journal of Physics: Conference Series, 2017, 950, 042050.	0.3	2
83	Spin Crossover and the Magnetic P–T Phase Diagram of Hematite at High Hydrostatic Pressures and Cryogenic Temperatures. JETP Letters, 2018, 107, 247-253.	0.4	2
84	Electron-withdrawing effect of α-substituents in acyl nitrates on the polarization of the O–NO2 bond. Mendeleev Communications, 2018, 28, 641-643.	0.6	2
85	Pressure-Induced Structural Transition to the Polar Phase in GdFe ₃ (BO ₃) ₄ . Crystal Growth and Design, 2019, 19, 6935-6944.	1.4	2
86	Synthesis and mutual transformations of nitronium tetrakis(nitrooxy)- and tetrakis(2,2,2-trifluoroacetoxy)borates. New Journal of Chemistry, 2020, 44, 13944-13951.	1.4	2
87	Pressure Induced Spin Crossover and Magnetic Properties of Multiferroic Ba3NbFe3Si2O14. Molecules, 2020, 25, 3808.	1.7	2
88	Structural transitions in iron-based Ba 3 NbFe 3 Si 2 O 14 langasite at high pressures. Europhysics Letters, 2016, 116, 66003.	0.7	1
89	Crystal structure and phase transitions at high pressures in the superconductor FeSe0.89S0.11. Journal of Alloys and Compounds, 2021, 860, 158419.	2.8	1
90	Crystal structure of the new superconductor FeSe1â^'x S x. Acta Crystallographica Section A: Foundations and Advances, 2017, 73, C525-C525.	0.0	0